Bioresource Technology 393 (2024) 130071

Contents lists available at ScienceDirect

Bioresource Technology

journal homepage: www.elsevier.com/locate/biortech

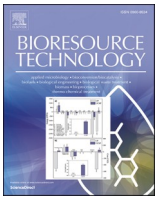

Processing of hemicellulose in wheat straw by steaming and ultrafiltration – A novel approach

Stanislav Parsin *, Martin Kaltschmitt

Hamburg University of Technology (TUHH), Institute of Environmental Technology and Energy Economics (IUE), Eissendorfer Strasse 40, 21073 Hamburg, Germany

HIGHLIGHTS

- Hydrolysis of wheat straw by saturated steam without rapid decompression.
- Hemicellulose hydrolysate with low particle and lignin load.
- High recovery of hemicellulose as xylooligosaccharides and xylan.
- High ultrafiltration flow rates at moderate conditions.
- A simple approach to a green process for the valorization of hemicellulose.

GRAPHICAL ABSTRACT

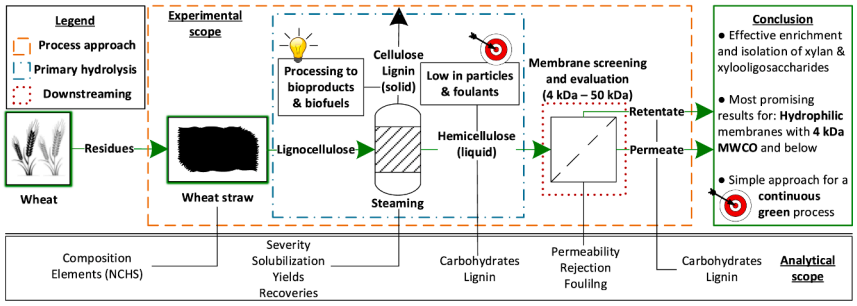

ARTICLE INFO

Keywords:
Hemicellulose
Wheat straw
Steaming
Ultrafiltration
Xylooligosaccharides

ABSTRACT

Water-soluble xylans useable for many potential applications can be produced based on the hydrolysis of wheat straw within a fixed bed using saturated steam to provide a xylan-rich hydrolysate low in particles and lignin enabling an effective ultrafiltration and xylan separation. Under defined conditions (180 °C, 10 bar, 35 min), a degree of solubilization of 29.6 % for straw and of 63 % for hemicellulose is achieved. The dry mass of the resulting hydrolysate consists of at least 58 % xylose and arabinose. The xylose is mainly (87 %) present in non-monomeric form and appears to have a broad molecular weight distribution. Ultrafiltration with commercial membranes (4 to 50 kDa) is being investigated for the separation of the target fraction; here significant differences in the filtration behavior and rejections from 9 to 81 % for carbohydrates and from 13 to 48 % for phenolic compounds (lignin), respectively, are found.

1. Introduction

So far, biorefineries have focused on fractionating lignocellulose (i.e., separating lignin, cellulose and hemicellulose) and then providing the simplest possible carbohydrates for further processing into, for example, ethanol or other bulk and/or fine chemicals (Gírio et al., 2010; Carvalheiro et al., 2008). This is especially true for hemicellulose; on the other hand, many applications for cellulose as a polymer already exist. Nevertheless, some of these biorefinery concepts have not proven themselves under commercial conditions, as for products for the energy market (i.e., electricity, heat or fuels) and for platform chemicals the competition on the markets is significant. In this respect, high value-added byproducts can improve the economics of such biorefineries (Scapini et al., 2021). Biopolymers from hemicellulose can be such a

* Corresponding author.
E-mail address: stanislav.parsin@tuhh.de (S. Parsin).

https://doi.org/10.1016/j.biortech.2023.130071
Received 14 August 2023; Received in revised form 13 November 2023; Accepted 17 November 2023
Available online 23 November 2023

side-product with a high added value e.g. for the food, the chemical and/or the pharmaceutical industry (Amorim et al., 2019; Ebringerová 2005). With suitable processes the heterogeneous hemicellulose components can be isolated from the biogenic feedstock in oligo- and polymeric form to be ready for a large number of possible applications already established on the market or being researched (Ebringerová 2005; Amorim et al., 2019; Naidu et al., 2018).

Lignocellulose being the feedstock for such a biorefinery approach is produced in considerable quantities for example as a byproduct in agriculture. One example of this is wheat straw being often not used effectively or not used at all (Jacquemin et al., 2012). This straw is characterized by a high global availability without causing additional arable land utilization and/or competition with food production. In addition, technologies for harvesting, logistics and processing as well as the necessary infrastructure are already established and widespread.

The hemicellulose in wheat straw consists mainly of xylan characterized by a backbone composed of β-1, 4-D-xylose linked subunits with different side chains (Ebringerová 2005). Xylan in hemicellulose is more amorphous and less resistant than cellulose (Gómez et al., 2015; Ibbett et al., 2011; Ebringerová 2005). High-polymer xylan is not soluble in water. Currently it is provided mainly by alkaline extraction from the lignocellulose structure (Santibáñez et al., 2021; Naidu et al., 2018; Kim et al., 2016). Lower molecular weight xylooligosaccharides (XOS), according to the most widely used definition, have a degree of polymerization (DP) of 2 till 10 and are mainly produced enzymatically (for a high purity and a low polydispersity) after an appropriate pretreatment (Aachary and Appukuttan, 2011; Santibáñez et al., 2021).

Xylooligosaccharides (XOS) are being researched in various medical contexts and can be used, for example, as a prebiotic food ingredient and as a substitute for inulin (in case of fructose intolerance) (Aachary and Appukuttan, 2011; Amorim et al., 2019). Xylooligosaccharides (XOS) / water soluble xylans (WSX) from different sources could lead to different therapeutic effects and some could replace the problematic FODMAP (Fermentable Oligo-, Di-, Monosaccharides and Polyols) compounds (So et al., 2021; François et al., 2014). In addition, xylooligosaccharides (XOS) can also contribute to the feed market to improve animal welfare (Qaseem et al., 2021). For monogastric animals, butyrate and propionate formation can be increased and a reduction of intestinal pathogens can be achieved. The use in case of diarrhea and for improved mucosal regeneration is suggested (Dotsenko et al., 2018; So et al., 2021). Various other potential applications in the cosmetics, healthcare and pharmaceutical industries are discussed (Naidu et al., 2018; Amorim et al., 2019; Qaseem et al., 2021).

The main challenge in the material utilization of wheat straw is the selection of a suitable pretreatment to break down and utilize the resistant structural biomass under reasonable conditions (Andersen et al., 2022; Bhutto et al., 2017). Various pretreatment methods (physical, chemical, physicochemical) have been investigated in the last decades (Santibáñez et al., 2021; Klemm et al., 2020). Of these, the alkaline and thermal (autohydrolysis and steam-based) methods are particularly suitable for recovering the hemicellulose fraction in oligomeric or polymeric form (Amorim et al., 2019; Carvalheiro et al., 2008; Scapini et al., 2021). Thermal processes such as autohydrolysis and steam explosion are considered to be environmentally friendly, since apart from water and energy no auxiliary materials are required and continuous operation (within limits) with high solids loading and short residence times is possible (Modenbach and Nokes, 2012; Wang et al., 2013). However, these processes also have disadvantages. Autohydrolysis with hot water allows high recoveries of hemicellulose in oligomeric form, but is very energy-intensive and runs at relatively high pressures (Ruiz et al., 2020; Santibáñez et al., 2021). In addition, the scalability is limited and the hydrolysate is heavily contaminated with phenolic compounds and particles due to a convective flow through the biomass (Bhutto et al., 2017; Zabed et al., 2016; Ruiz et al., 2020; Montané et al., 2006). Thus, for cost effective commercial processing of lignocellulose, severe conditions, expensive materials, high energy consumption, catalysts and auxiliary reagents should be avoided (Bhutto et al., 2017).

From today's point of view, steam processes offer the most promising conditions for the efficient production of oligomers and polymers from hemicellulose on an industrial scale (Ruiz et al., 2020). However, there is still a need for optimization. Besides the typically high heat demand, steam-based processes are in general not selective for specific target fractions (Bhutto et al., 2017; Li et al., 2007). Due to the crystallinity of cellulose, an effective solution in water below 210 °C is difficult to realize (Dogaris et al., 2009). However, hemicellulose and lignin are subject to degradation and condensation reactions even at temperatures below 200 °C (Li et al., 2007; Sun et al., 2005). As a result, various reactions take place in parallel (Li et al., 2007,2005; Scherzinger and Kaltschmitt, 2021). For example, carbohydrates are degraded via the monosaccharides to aldehydes and organic acids (Li et al., 2005). Lignin is partially degraded to phenolic compounds (Li et al., 2007). Recombination reactions of reactive molecules also occur (Scherzinger and Kaltschmitt, 2021). This often results in a complex hydrolysate demanding an expensive downstream processing (Bhutto et al., 2017; Hongzhang and Liying, 2007). In this respect, membrane filtration can be an effective solution, especially to isolate high value oligomers and polymers and at the same time to achieve the current goals of a circular economy with less waste generation (Scapini et al., 2021; Bhutto et al., 2017).

So far, steam explosion has mainly been used to break down the resistant structure of lignocellulose in thermal pretreatment (Bhutto et al., 2017). This method is considered to be state of the art for thermal decomposition of lignocellulose and is already being implemented at various scales (Ruiz et al., 2020). Although it was shown decades ago that the benefit of sudden decompression at the end of the steam explosion (depending on biomass type and process conditions) is debatable (Brownell and Saddler, 1987). Compared to that a pure steam treatment without realizing an explosion at the end of the treatment is rarely dealt with in literature and if only to a minor aspect (Ruiz et al., 2020). Luo et al., for example, avoided the explosion in order to investigate the influence of temperature on the degradation kinetics of hemicellulose in green bamboo (Luo et al., 2013). Schütt et al. compared steam explosion and steam refining on poplar wood chips (for enzymatic accessibility) and concluded that the explosion is not necessary (Schütt et al., 2012). Often dry biomass is used in such investigations and no differentiation is made between saturated and superheated steam. Only few examples exist for the use of saturated steam for the treatment of moist lignocellulose aiming in a fractionation of the various biomass components. Steinbrecher et al., for example, realized a thermal hydrolysis of biogas residues with saturated steam within the lab-scale in order to use the remaining carbohydrates in the residue more effectively (Steinbrecher et al., 2022).

Especially for herbaceous biomass, the benefit of the rapid decompression at the end of the steam explosion process is questionable, because the available surface area of herbaceous biomass is large anyway and the rapid decompression complicates a recycling of the steam (i.e., decreases the overall energy efficiency). Rodriguez et al. concluded that the abrupt decompression for the subsequent enzymatic degradation becomes significant only at a temperature of $\geq$ 220 °C for wheat straw (Rodríguez et al., 2017). The results also suggest that the parameters temperature and reaction time are decisive beforehand and that only above a threshold value of 220 °C the necessary energy is applied to decompose the still remaining 5 to 10 % crystalline cellulose (at low enzyme loadings). Thus, lower temperatures would lead to lower final glucose yields in the produced hydrolysate. However, this does not necessarily need to be critical for a respective biorefinery concept, if the overall costs are lower at the end, losses associated with lower glucose yields can be (over)compensated (Andersen et al., 2022). Moreover, decomposition of the hemicellulose fraction already takes place at significantly lower temperatures (Ruiz et al., 2020).

If the target fraction for solubilization occurs exclusively in the cell

wall (i.e., structural biomass), it could be counterproductive for the downstreaming to disrupt the cells as completely as possible and to release the intracellular compounds (Biswas et al., 2011). Thus, if only the hemicellulose is to be solubilized in the pretreatment, the plant cell walls should not be inevitably decomposed by explosion. Instead, a steady release of steam might help to remove the hemicellulose components from the organic matter and allow recycling of the steam in parallel (i.e., reduction of the thermal energy demand). Coupled with mechanical instead of thermal processes within the downstream processing, typical drawbacks (i.e., high thermal energy consumption and costly downstream processing of products) could be at least partially overcome (Ruiz et al., 2020; Bhutto et al., 2017). Ultrafiltration, together with effective steam pretreatment and recycling, can help to combine the holistic utilization of wheat straw with the necessary multi-product concept for a viable biorefinery (Scapini et al., 2021).

So far, there is a lack of feasible approaches for the industrial and continuous production of water-soluble xylans from the hemicellulose fraction in integrated biorefinery concepts (Scapini et al., 2021). Such an approach must combine established scalable technologies (for cellulose and lignin) with the production of water-soluble xylans in a way that is as efficient, competitive and feasible on a large scale as a green process (Scapini et al., 2021; Ruiz et al., 2020). The combination of steaming and ultrafiltration is one possible approach. However, the interactions during ultrafiltration need to be studied in detail and the primary hydrolysis needs to be adapted for ultrafiltration to avoid the problems described (i.e. potentially high energy demand and high costs) (Ruiz et al., 2020; Bhutto et al., 2017). In this way, the wheat straw biomass can be successfully broken down for further processing (e.g., into biofuels) and the hemicellulose becomes a byproduct with high economic value. Against this background, the aim of this work is to investigate and evaluate the separation of oligomers and polymers from wheat straw hydrolysates by ultrafiltration provided by steaming of the moist feedstock. Therefore, wheat straw is treated with saturated steam (without rapid decompression at the end) for solubilizing the hemicellulose fraction (the utilization of cellulose and lignin is not considered further here). The resulting hemicellulose hydrolysate is then analytically characterized. The goal of the primary hydrolysis is the provision of a hydrolysate being suitable for ultrafiltration under moderate conditions (i.e., low transmembrane pressure and temperature). The hydrolysate is subsequently used as feed for ultrafiltration with suitable and commercially available membranes. Various polysulfone-based membranes with a molecular weight cut-off (MWCO) between 4 and 50 kDa are screened, since the molar mass distribution of the target carbohydrates is not yet known. During filtration, characteristic process parameters such as carbohydrate and lignin retention, permeability and membrane fouling are determined. The results allow to find the most suitable solution for the effective filtration of the hydrolysates produced, depending on the membrane properties (e.g., pore size, zeta potential and hydrophobicity).

2. Materials and methods

In the following section, the used materials as well as the experimental and analytical methods are described. A graphical overview of

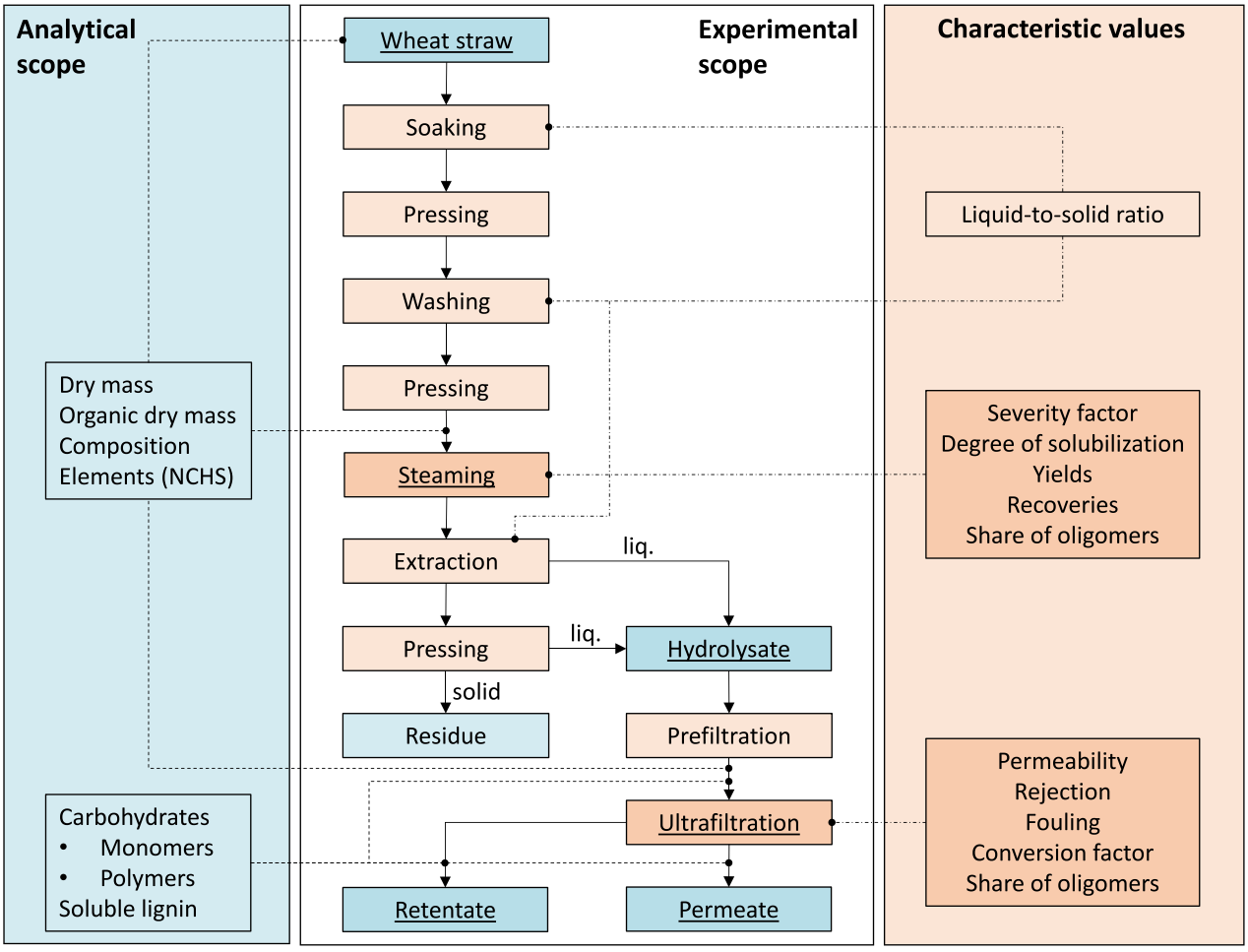

Fig. 1. Experimental and analytical procedure and the defined characteristic values. Experimental process steps are shown in orange and fractions/intermediates in blue. The main objects of investigation are underlined.

the experimental and analytical procedure with associated characteristic values shows Fig. 1.

2.1. Feed biomass

The wheat straw (WS) was harvested in the year 2020 in Grasberg (Lower Saxony, Germany) and provided by the company Cordes-Grasberg (Grasberg, Germany). The wheat straw was supplied dedusted and chopped to an edge length of about 1 cm.

2.2. Primary hydrolysis (steaming)

In the following, the experimental procedure and the defined characteristic values of the primary hydrolysis are explained.

2.2.1. Experimental procedure

Wheat straw was soaked with 60 °C hot tap water (water bath) at a liquid-to-solid ratio of 20 for 20 min before each primary hydrolysis. During this wetting the container was stirred. Subsequently, the wet straw was pressed off. A 40 L hydropress (Wiltec Wildanger Technik GmbH, Eschweiler, Germany) was used for squeezing the straw-water-mixture at 3 bar pressure. The biomass was then rinsed with deionized water and squeezed again with the same press. The wash water was sampled (pH-value, turbidity and HPLC analysis according to section 2.4) and subsequently discarded. The steam treatment (primary hydrolysis) took place in a 40 L (void volume) high pressure fixed bed reactor made of stainless steel (Fig. 2). The cylindrical reactor was preheated to 180 °C via the heating jacket using an oil heater with an installed power of 18 kW (TT-390 Z, Tool-Temp AG, Sulgen, Switzerland). In addition, the interior was heated with saturated steam from deionized water at 180 °C provided by a 15 kW steam generator (model 200–15, Stritzel Dampftechnische Geräte GmbH, Mülheim an der Ruhr, Germany). The condensate was subsequently drained. The washed biomass (typically 2 to 3 kg) was evenly distributed within a removable stainless steel cartridge without pressing. The cartridge is a cylinder made of steel with screw-in sieves as base and top surface to pass steam and water through it. Once a constant temperature was reached, the cartridge containing the biomass was placed into the preheated reactor with a chain winch. The outlet valve and the steam inlet valve (Fig. 2) were opened and saturated steam was slowly introduced from top to bottom to preheat the biomass and displace the air contained originally within the reactor (5 to 10 min). The resulting condensate was discarded until both reactor temperature sensors (Fig. 2) indicated at least 100 °C. The outlet valve was closed and the steam supply from the steam generator (15 kW) was maximized (fully opened valves). The measured reaction time started as soon as the absolute pressure in the reactor reached 9.9 bar. Start criterion for the measured reaction time was ca. 1 % deviation of the set value at 10 bar (steam pressure at 180 °C). After 35 min measured reaction time, the steam supply was stopped and both outlet valves (Fig. 1) were opened.

The pressure (and thus the temperature) in the reactor was then continuously reduced to atmospheric pressure (typical duration: 50 to 120 s). Afterwards the biomass was removed for extraction and analysis. The process parameters (*p, T, t*) were monitored and displayed digitally. The control was manual.

The removed pretreated hot biomass was then extracted with

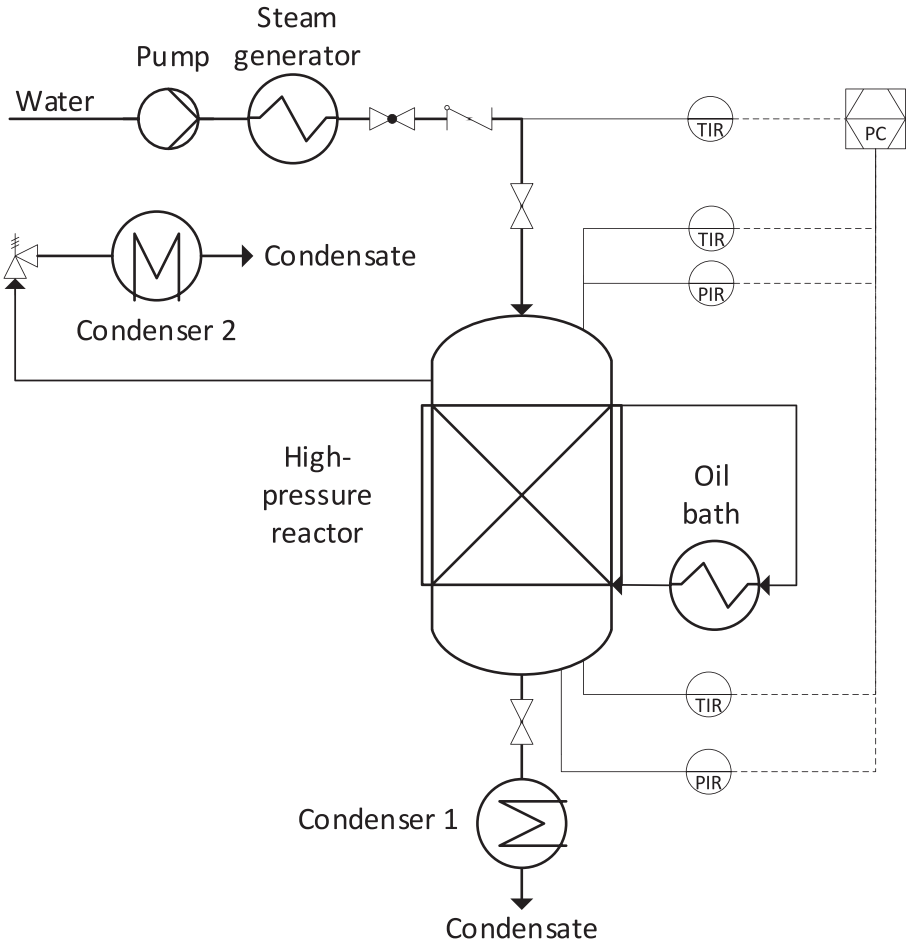

Fig. 2. Illustration of the 40 L reactor for primary thermal hydrolysis (applied conditions: $T = 180$ °C; $t = 35$ min; $p = 10$ bar; TIR = temperature indicator recorder; PIR = pressure indicator recorder).

deionized water (20 °C) in the cartridge for 15 min at a liquid-to-solid ratio of 3. The extract was collected. Because most of the water was absorbed by the biomass, the wet biomass was transferred into the 40 L hydropress (Wiltec Wildanger Technik GmbH, Eschweiler, Germany) and pressed at a pressure of about 3 bar (through a sieve with a mesh size of 1 x 5 mm). The pressed liquid phase was mixed with the extract to form the provided hydrolysate as indicated in Fig. 1. The remaining soluble biomass on the solid residue was washed off with tap water (until the effluent was completely clear) to determine the degree of solubilization (Equation (2.4)). The wash water was sampled and discarded.

Samples of the hydrolysate, the solid residue, the washing water and the condensate were taken for mass balances and analysis (section 2.4) and stored frozen (- 20 °C) or freeze-dried. The hydrolysate was stored frozen until ultrafiltration. Losses due to the non-condensed gas phase were neglected. The primary hydrolysis experiments were performed in triplicates.

2.2.2. Characteristic values

For comparison of reaction conditions and treatment concepts for lignocellulose, characteristic values are defined (Fig. 1).

For the quantification of the amount of solvent (e.g., water for soaking, washing or extraction), it is related to the dry mass. Based on this the so-called liquid-to-solid ratio is formed according to Equation (2.1). Here, for the liquid-to-solid ratio for a process step j, the mass of the liquid phase (m_j^l in g) (1 kg = 1 L, as only water is used) is divided by the dry mass of the solid sample (m_j^s in g) after 105 °C drying.

$$\frac{L}{S_j} = \frac{m_j^l}{m_j^s} \tag{2.1}$$

To quantify the severity of a treatment step a dimensionless severity factor is defined (Li et al., 2007,2005; Scherzinger and Kaltschmitt, 2021). With the temperature (T in °C) and time (t in min) dependent reaction ordinate R_0 in Equation (2.2), the applied conditions correspond to a severity factor S_0 (Equation (2.3)) of 3.9.

$$\log_{10}(R_0) = \log_{10}\left(t \exp\left(\frac{T(t) - 100}{14.75}\right)\right) \tag{2.2}$$

$$S_0 = \log_{10}(R_0) \tag{2.3}$$

The degree of solubilization (DS) (in %) for the solid biomass (Equation (2.4)) is calculated with the initial dry weight of the solid dry biomass before (m_0^s in g) and after (m_1^s in g) the treatment step.

$$DS_{th} = \frac{m_0^s - m_1^s}{m_0^s} 100 \tag{2.4}$$

The recovery ($Rec_{i,j}$ in %) of a certain component i in the liquid sample ($m_{i,j}^l$ in g) derived from the solid biomass ($m_{i,j-1}^s$ in g) after a process step j is calculated according to Equation (2.5). Here, the measured concentration of the component i in the liquid phase after the step ($c_{i,j}^{total}$ in g/L) is determined in the total volume of the reaction product (V_R in L) and linked to the factor for the anhydro correction (AC). To determine the recovery, the term is divided by the product of the initial solid mass before the step (m_{j-1}^s in g) and the solid mass fraction of component i in it ($w_{i,j-1}$ in %).

$$Rec_{i,j} = \frac{m_{i,j}^l}{m_{i,j-1}^s} = \frac{c_{i,j}^{total} V_R AC}{w_{i,j-1} m_{j-1}^s} \tag{2.5}$$

The yield of a dissolved component i is calculated based on its total mass in the liquid fraction (m_i^l in g) and the initial solid biomass (m_0^s in g) or its total recovery in the liquid phase after thermal hydrolysis ($Rec_{i,th}$) following Equation (2.6). The recoveries and yields are calculated by means of the analytical methods (section 2.4).

$$Y_i = \frac{m_i^l}{m_0^s} = Rec_{i,th} w_{i,0} \tag{2.6}$$

Consequently, a share of oligomers S_i^{ol} (in %) for a measured component i in the hydrolysate was defined according to Equation (2.7). Here, c_i^{mono} (in g/L) is the measured concentration of the monomeric component i in the sample and c_i^{total} (in g/L) is the total concentration of the component i after analytical hydrolysis (including anhydro correction according to section 2.4.2).

$$S_i^{ol} = \left(1 - \frac{c_i^{mono}}{c_i^{total}}\right) 100 \tag{2.7}$$

2.3. Ultrafiltration

In the following, the experimental procedure and the defined characteristic values of the ultrafiltration experiments are explained.

2.3.1. Experimental procedure

For ultrafiltration, the membranes listed in the Table 1 were screened after preselection (membranes were selected with regard to cost, process parameters and availability). For all ultrafiltration experiments the hydrolysate of one primary hydrolysis batch was used as feed. The hydrolysate was filtered by vacuum filtration through a 5 µm cellulose acetate filter (Sartorius Stedim Biotech GmbH, Göttingen, Germany) to separate coarse impurities and particles after cooling down.

For the isolation of xylan, an ultrafiltration unit with data acquisition, consisting of 400 mL dead-end filtration cells (Amicon 8400, Millipore Corp., Billerica, MA, USA) with the setup shown in Fig. 3, was used. All flat-sheet membranes (for specifications see Table 1) were prepared according to the instructions of the respective manufacturer and soaked in deionized water for 24 h before the experiments. During filtration the three cells (triplicates) were placed on magnetic stirrers and connected to the nitrogen bottle via pressure hoses. The permeates produced in each case were collected in vessels placed on individual scales; the mass change was recorded continuously. LabVIEW software (2019 SP1) was used to process and record the measured values.

All experiments were performed with unused and freshly prepared membranes. The membranes have an active filtration area of 45 cm^2. The transmembrane pressure (TMP) of 1 to 4 bar (depending on the molecular weight cut-off) as the driving force of the filtration was adjusted with a pressure reducer. The transmembrane pressure is therefore the difference to the atmospheric pressure on the permeate side. The cells were constantly stirred (150 min^{-1}) at 20 to 22 °C during filtration to counteract concentration polarization.

For the experimental study, the following steps were performed with each new membrane:

Step 1. Filtration of 200 g deionized water (5 x) to determine the virgin permeability (Equation (2.9)).

Step 2. Filtration of 100 g hydrolysate sample until 50 % is converted to permeate (Equation (2.10)).

Step 3. Filtration of 200 g deionized water to determine the permeability of the fouled membrane (reversible + irreversible fouling).

Step 4. Turning the membrane.

Step 5. Backwashing with 100 g deionized water (2 x).

Step 6. Turning the membrane again.

Step 7. Filtration of 200 g to determine the permeability of the rinsed membrane (irreversible fouling).

The generated data is used to calculate the characteristic values defined in section 2.3.2. Samples of the feed, permeates and retentates were taken for mass balances and analysis (section 2.4) and stored frozen (- 20 °C). The ultrafiltration experiments were performed in triplicates.

Table 1
Investigated membranes with information on the manufacturers and typical operating conditions according to the distributers.

Membrane type	MWCO[a] kDa	Material[b]	Supplier	pH	*T* °C	*p* bar	Permeability[c] L/(m² h bar)
UH050	50	Hydrophilic PES	MN	0–14	5–95		≥ 85
UH030	30	Hydrophilic PES	MN	0–14	5–95		≥ 35
UP020	20	PES	MN	0–14	5–95		≥ 70
UP010	10	PES	MN	0–14	5–95		≥ 50
UP005	5	PES	MN	0–14	5–95		≥ 10
UH004P	4	Hydrophilic PES	MN	0–14	5–95		≥ 7.0
UF10	10	PES	MN	2–11	5–45	1–21	≥ 74
UF5	5	PES	MN	2–11	5–45	1–21	≥ 8.3
PS (GR61PP)	20	PS	AL	1–13	5–75	1–10	
PES (GR80PP)	10	PES	AL	1–13	5–75	1–10	
PES (GR90PP)	5	PES	AL	1–13	5–75	1–10	

[a] MWCO, nominal molecular weight cut-off.
[b] PES – Polyethersulfone, PS – Polysulfone.
[c] for respective test conditions.

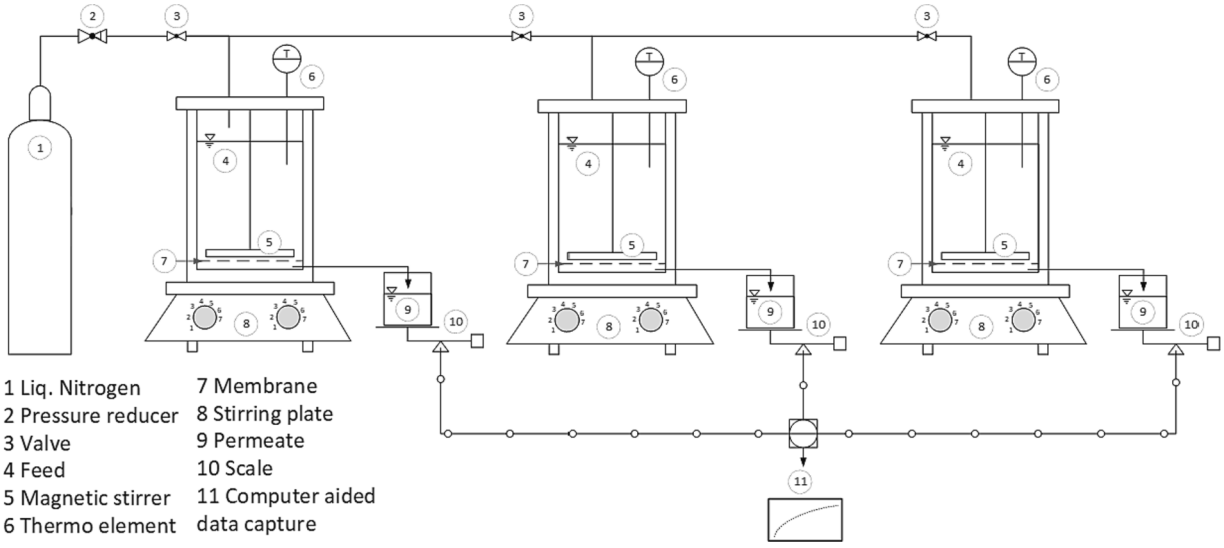

Fig. 3. Experimental setup for ultrafiltration (transmembrane pressure 1 to 4 bar).

2.3.2. Characteristic values

For the comparison of the membranes and the reproducibility of the results, characteristic values outlined below were defined (Fig. 1).

The permeate flux ($\dot{J}$ in L/(m² h)) of each membrane was determined according to Equation (2.8). The density of the permeate was assumed to be constant with a value of 1 kg/L (empirical, densities of 1.013 till 1.021 kg/L were measured for the feed/hydrolysate).

$$\dot{J} = \frac{\Delta V^{Per}}{A_m \Delta t} \tag{2.8}$$

The flux for a certain period (Δt in h) can be calculated from the permeate volume difference (ΔV^{Per} in L) and the active membrane area (A_m in m²). To compare membranes at different operating pressures, the flux is normalized for the transmembrane pressure (*TMP*) and the permeability ($\dot{P}$ in L/(m² h bar)) is calculated according to Equation (2.9).

$$\dot{P} = \frac{\Delta V^{Per}}{A_m \Delta t TMP} \tag{2.9}$$

In order to compare the filtration results of different membranes for the hydrolysate samples, a conversion factor (*CF* in %) was defined according to Equation (2.10). The filtration of the hydrolysate continues until the conversion (feed (m^{Feed} in g) to permeate (m^{Per} in g)) of 50 % is reached and is then stopped.

$$CF = \frac{m^{Per}}{m^{Feed}} 100 \tag{2.10}$$

Membrane fouling can be quantified according to the procedure defined in section 2.3.1. The reversible, the irreversible and the membrane fouling for sample filtration (i.e., reduction of permeability) are calculated by means of the permeabilities after

- (Step 2) filtration of the sample,
- (Step 3) filtration of deionized water with a fouled membrane and
- (Step 7) filtration of deionized water after backwashing.

The membrane fouling (*F* in %) is calculated as a quotient from the permeability after a process step *j* ($\dot{P}_j$ in L/(m² h bar)) and the initial permeability for deionized water (DIW) of the virgin membrane ($\dot{P}_o^{DIW}$ in L/(m² h bar)) according to Equation (2.11).

$$F_{irr\backslash rev\backslash sample} = \left(1 - \frac{\dot{P}_j}{\dot{P}_o^{DIW}}\right) 100 \tag{2.11}$$

To assess the retention of a membrane for a given component *i* (e.g., non-monomeric xylose), the so-called rejection (R_i in %) is calculated using the measured concentrations (c_i in g/L) in the feed and permeate according to Equation (2.12). For the rejection calculation of sugars, the

methods described in section 2.4.2 and 2.4.3 were used.

$$R_i = \left(1 - \frac{c_i^{Per}}{c_i^{Feed}}\right) 100 \quad (2.12)$$

For the rejection calculation of soluble lignin (Equation (2.13)), the methods described in section 2.4.4 were used.

$$R_{Lig} = \left(1 - \frac{Abs_{760}^{Per}}{Abs_{760}^{Feed}}\right) 100 \quad (2.13)$$

The relative lignin content (C_{Lig}^{Rel} in %) (Equation (2.14)) was determined using the absorbances of the samples (Abs_{760}^{Sample}) and the feed (Abs_{760}^{Feed}) at 760 nm wavelength according to the method described in section 2.4.4.

$$C_{Lig}^{Rel} = \frac{Abs_{760}^{Sample}}{Abs_{760}^{Feed}} 100 \quad (2.14)$$

The share of oligomers S_i^{ol} (in %) for a measured component i in the retentate or permeate was defined according to Equation (2.7).

2.4. Analytical methods

Below the analytical methods being used, developed, or adapted for component identification and balancing are described. Ultrapure water with a maximum conductivity of 0.05 µS/cm was used for the analytical procedures. The chemicals used for the analytical procedures according to the referenced literature were of analytical grade.

2.4.1. Compositional analysis

The chemical composition analysis of the feedstock and solid biomasses was conducted according to the NREL guideline LAP TP-510–42618 (A. Sluiter et al., 2011). The dry weight of the acid-insoluble lignin was corrected with respect to the ash content for compositional analysis. The organic dry mass content of the liquid and solid samples was determined according to the DIN EN ISO 18122 standard at 550 °C (DIN EN ISO, 2015). The main elements (nitrogen, carbon, hydrogen and sulfur) of the samples were determined using a NCHS elementary analyzer (Vario Macro Cube, Langenselbold, Germany). The protein content was subsequently calculated by multiplying the nitrogen content by a factor of 6.25, since a standard protein contains 16 % nitrogen (Helmut Diedrich, 2019).

2.4.2. Quantification of carbohydrates (HPLC)

A high-performance anion exchange chromatography with refractive index detector (HPAEC-RID) (Agilent 1260 Infinity II, Agilent, Santa Clara, CA, USA) was used for the quantification of di- and monomeric carbohydrates, organic acids and degradation products (5-hydroxymethylfurfural (HMF) and furfural). In combination with the analytical column Hi-Plex H^+ (Agilent, Santa Clara, CA, USA) and a mobile phase of ultrapure water with 5 mM H_2SO_4, the relevant monosaccharides (D(+)glucose, D(+)xylose and L(+)arabinose) and the disaccharides D-cellobiose and D-xylobiose can be determined in a single run. Since peak overlaps often occur due to coelution of compounds in complex samples, the results were additionally verified with a Hi-Plex Pb^{2+} column (Agilent, Santa Clara, CA, USA). For the analysis with the Hi-Plex H^+, a flow rate of 0.5 mL/min in isocratic mode and an injection volume of 10 µL were set. The temperature of the column and the detector was 55 °C. For the evaluation, a seven-point calibration for all analyzed compounds was performed in the measuring range.

The calculations of the yields and the recoveries for the released respective component from the detected concentrations were performed according to the NREL LAP TP-510–42618 with respect to anhydro corrections (*AC*) (A. Sluiter et al., 2011). Additionally, a correction factor of 0.978 is used for formic acid, as the results suggest that it is released from formates in the biomass during primary hydrolysis.

2.4.3. Quantification of oligomeric and polymeric carbohydrates

The content of components in liquid phases released from oligomers or polymers was determined indirectly as difference after hydrolysis to monomers according to the NREL protocol (Sluiter, 2008). For this, so-called analytical hydrolysis, 10 mL of each liquid sample was sterile filtered (0.45 µm) and hydrolyzed after addition of H_2SO_4 at 121 °C for 60 min (Thermoreactor TR420, Merck, Germany). The hydrolysis to monomers should proceed as completely as possible without forming unwanted degradation products. Therefore, the amount of H_2SO_4 was adjusted from 4 to 2 wt-% after optimization of the recovery (comparable to (Beckendorff et al., 2021)). The hydrolyzed samples were then analyzed by HPAEC-RID and the yields and recoveries were calculated by the method described in the protocol TP-510–42618 (A. Sluiter et al., 2011). The difference between the measured concentrations of the analytes before and after analytical hydrolysis can be used to calculate the respective share of oligomers in a sample (Equation (2.7)).

2.4.4. Soluble lignin analysis

The quantification of dissolved lignin in liquid samples was carried out according to TP-510–42618 (A. Sluiter et al., 2011). The dissolved lignin content was determined by UV spectroscopy at a wavelength of 320 nm and a specific absorptivity constant of 30 L/(g cm) in particle free samples (0.45 µm filtration). Prior to the determination, furfural was removed from the sample by vacuum distillation, since it has a high extinction coefficient in the wavelength range applied. Furfural at low concentrations in water behaves as light end during distillation despite having a higher boiling point. The volume loss of water and furfural was then compensated by adding pure water to avoid falsifying the composition. HMF also has a high specific extinction coefficient at 320 nm wavelength. But, HMF was neglected because the controls via HPLC did not show a sufficiently high concentration for the evaluation.

For samples after ultrafiltration, the relative lignin content in the fractions (permeate and retentate) was determined in relation to the feed using Folin-Ciocalteu reagent according to the Dual Reagent Method (Agbor, 2014). The absorbance was measured after 2 h reaction time in the absence of light, and the relative lignin content was calculated according to Equation (2.14). With this method the lignin content is determined by UV/Vis spectroscopy after the reaction of the reducing functional groups (mainly C-C double bonds) with the reagent. Thus, the relative lignin content is identified by the amount of dissolved phenolic components. The lignin content tends to be overestimated, since compounds such as furfural and HMF are also involved in the reaction. However, these are only included by their amount of substance and not by their specific extinction coefficient. Thus, the method is much less susceptible to fluctuations due to these degradation products of the sugars.

2.4.5. Turbidity

The turbidity of the liquid samples (hydrolysate, permeate, retentate) was measured in the infrared range using the P2100P ISO meter (Hach Lange GmbH, Düsseldorf, Germany). The measured values are expressed in NTU (*Nephelometric Turbidity Units*) relative to standard solutions of formazin after calibration in the range of 0.01 and 1750 NTU.

3. Results and discussion

In the following, the experimental results are presented and discussed.

3.1. Primary hydrolysis (steaming)

In the following, the results related to the solubilization of wheat straw and the resulting hydrolysate after steaming using the parameters defined in Fig. 1 are presented and discussed.

3.1.1. Wheat straw solubilization

Results. Primary hydrolysis with saturated steam resulted in effective liquefaction of the hemicellulose. The composition of the solid biomass before and after treatment with saturated steam changes considerably, as some of the solids solubilize by forming the hydrolysate. The results of the analytical investigations are summarized in Table 2. Recoveries (Equation (2.5)) and yields (Equation (2.6)) of the respective fraction are reported for the hydrolysate dry mass under the conditions selected (section 2.2.1).

The raw straw has a dry mass of 90.9 ± 0.2 wt%. After washing, the moisture content increased to 37.1 ± 0.2 wt%. Washing increases the relative organic dry mass (oDM) content from 92.1 ± 0.1 wt% to 94.1 ± 0.1 wt%, since inorganic salts are removed (but also organic components, since the total losses of dry mass are greater than the salt losses).

For the hydrolysis with saturated steam, the moisture of the biomass was found to have a major influence on the result. Under the selected conditions, the degree of solubilization during the primary thermal hydrolysis (DS_{th}) was 29.6 ± 0.4 %. Of the solubilized biomass, 49 % can be recovered in the hydrolysate dry mass using the experimental setup described in section 2.2.1 (corresponding to 14.5 % yield/recovery of the feed dry mass). Here, especially the liquid-to-solid ratio during the extraction is crucial (here $L/S = 3$). The rest of the liquefied biomass remains on the solid fraction and is washed off (supplementary data). The results show that mainly the fractions hemicellulose (reported as xylose, arabinose and furfural) and acetates are solubilized. In contrast, the hydrolysate dry mass consists mainly of hemicellulose (57.9 ± 1.2 wt% corresponding to 31.8 ± 1.1 % recovery and 8.4 ± 0.3 % yield for applied conditions), as the other fractions are not effectively liquefied and remain in the solid residue.

Discussion. If the goal is the provision of xylooligosaccharides (XOS) / water soluble xylans (WSX), high yields beyond the hemicellulose content in the biomass are unfavorable for primary hydrolysis. All other solubilized components besides hemicellulose (especially further biopolymers) most likely complicate downstream processing of the hydrolysate by means of ultrafiltration (Ruiz et al., 2020). The results of primary hydrolysis in Table 2 show that the liquefaction of the fractions that most interfere with the following ultrafiltration (i.e., cellulose, lignin and proteins) is low. It is important to emphasize that a number of milestones have been achieved with the process described (section 2.2.1). The soaking and (warm) washing of the straw reduces soluble extractables (rest) and ash in the biomass prior to hydrolysis, which are significant foulants in downstreaming. In addition, the necessary moisture is introduced into the biomass to support autohydrolysis and heat transport. It is important to achieve a water content above 50 wt%, otherwise primary hydrolysis will lead to different results (i.e., formation of monomers and degradation products). Without rapid decompression, less ash (17.5 ± 0.5 %) is solubilized compared to steam explosion (Biswas et al., 2011). It is also possible that pressing through the solid residue reduces the impurities in the hydrolysate. Comparatively high specific solubilization of hemicellulose is achieved, whereby no intensive straw preparation was carried out. The straw was merely chopped to an edge length of 1 cm by the manufacturer, which in fact can also mean up to 10 cm length (supplementary data). Size reduction (e.g., pelletizing) typically leads to better solubilization (Carvalheiro et al., 2008), but is disadvantageous from a process engineering point of view (Scapini et al., 2021; Bhutto et al., 2017). The low hemicellulose recoveries and yields for the hydrolysate in Table 2 are due to the poor extraction yield by the experimental setup described in section 2.2.1. A considerable part of the solubilized hemicellulose (over 50 %) is not extracted and is discharged with the washing water (supplementary data).

3.1.2. Wheat straw hydrolysate

Results. Primary hydrolysis with saturated steam results in a hydrolysate low in lignin and particles and a typical pH value of 3.8 to 4.1. The measured turbidities for the hydrolysates were in the range of about 50 to 100 NTU (section 2.4.5). Table 3 summarizes the results of the characterization of the produced hydrolysate by HPLC (section 2.4). The results show that the carbohydrates in the dry mass are mainly composed of xylose, arabinose and glucose being consistent with findings from literature (Ebringerová 2005). From the difference in concentration before and after analytical hydrolysis, the share of the respective analyte released from oligomers (S^{ol} according to Equation (2.7)) can be concluded. The results show that 87 % of the xylose in the hydrolysate is present in oligomeric form. For glucose in the hydrolysate, the share of oligomers is 95 %, which is even higher. Arabinose is largely released during the thermal pretreatment. Only 30 % of the total arabinose is bound in oligomers. For the degradation products HMF and furfural, the S^{ol} has a different meaning. These are not bound in oligomers and are rather formed via sugar degradation during analytical hydrolysis with added H_2SO_4. Formic acid is not formed in notable amounts during analytical hydrolysis, although it is present in the native hydrolysate in higher concentrations (0.80 g/L) than the degradation products HMF (0.10 g/L) and furfural (0.50 g/L). The oligomers in the hydrolysate are partially acetylated, since 26 % of the total acetic acid is released during analytical hydrolysis. After analytical hydrolysis, low concentrations of cellobiose are detectable, which indicates incomplete hydrolysis of at least stable compounds. Xylobiose, on the other hand, was not detected after analytical hydrolysis. The calculated arabinose (Ara) to xylose (Xyl) ratio in the native hydrolysate is 42.9 ± 0.2 % and

Table 2
Results and respective standard deviations (STD) for primary thermal hydrolysis with saturated steam according to section 2.2.1 (oDM = organic dry mass; WS = wheat straw; n. d. = not determined).

Fraction	DM	oDM	Cellulose	Hemicellulose	Lignin	Acetate	Ash	Protein	Rest[b]
Unit	$wt\%_{FM}$	$wt\%_{DM}$	$wt\%_{DM}$	$wt\%_{DM}$	$wt\%_{DM}$	$wt\%_{DM}$	$wt\%_{DM}$	$wt\%_{DM}$	$wt\%_{DM}$
Raw WS	90.9	92.1	31.3	24.2	18.6	4.5[d]	7.9	2.3	11.1
STD	0.2	0.1	1.3	0.9	0.4	0.2	0.1	0.1	1.7
Washed WS	37.1	94.1	32.2	26.4	20.5	5.0[d]	5.9	2.5	7.7
STD	0.2	0.1	0.5	0.9	0.2	0.1	0.1	0.1	1.1
Hydrolysate	4.5	93.0	5.5	57.9	6.8	7.1	7.0	2.3	13.3
STD	0.1	0.3	0.2	1.2	0.1	0.2	0.3	0.3	1.3
Solubilisation	29.6 %	30.3 %	3.5 %[c]	63.1 %	4.8 %[c]	70.8 %	17.5 %	13.5 %	24.9 %
STD	0.7 %	1.0 %	0.1 %	3.1 %	0.1 %	1.1 %	0.5 %	1.5 %	3.5 %
Recovery[a]	14.5 %	14.3 %	2.5 %	31.8 %	4.8 %	20.7 %	17.3 %	13.5 %	n. d.
STD	0.3 %	0.7 %	0.1 %	1.1 %	0.1 %	0.3 %	1.1 %	2.1 %	n. d.
Yield[a]	14.5 %	13.5 %	0.8 %	8.4 %	1.0 %	1.0 %	1.0 %	0.3 %	n. d.
STD	0.3 %	0.6 %	0.0 %	0.3 %	0.0 %	0.0 %	0.1 %	0.1 %	n. d.

[a] The yield and the recovery account for the specified components in the hydrolysate DM produced by the exp. setup described in section 2.2.
[b] The rest accounts for the unspecified components in the respective DM.
[c] Detected in the hydrolysate, not by compositional analysis.
[d] Without Soxhlet-extraction.

Table 3
Results and respective standard deviations (STD) of HPLC analysis of the investigated hemicellulose hydrolysate and condensate after hydrothermal pretreatment with saturated steam according to section 2.2.1.

HPLC results before analytical hydrolysis (monomers)									
Component	Cellobiose	Glucose	Xylose	Arabinose	Formic Acid	Acetic Acid	HMF	Furfural	Ara/Xyl
Unit	g/L	g/L	g/L	g/L	g/L	g/L	g/L	g/L	
Hydrolysate	0.00	0.08	3.36	1.44	0.80	2.41	0.10	0.50	42.9 %
STD	0.00	0.00	0.01	0.00	0.00	0.01	0.01	0.00	0.15 %
HPLC analysis after analytical hydrolysis (total)									
Hydrolysate	0.82	1.75	26.11	2.06	0.80	3.28	0.11	0.92	7.9 %
STD	0.01	0.06	0.08	0.02	0.00	0.02	0.01	0.03	0.07 %
Released from oligomers									
Hydrolysate	0.82	1.67	22.75	0.62	0.00	0.87	0.01	0.42	2.7 %
STD	0.01	0.06	0.07	0.01	0.00	0.02	0.00	0.03	0.06 %
S^{ol} (%)[a]	–	95	87	30	0	26	8	46	–
Condensate[b]	0.00	0.01	0.08	0.00	0.16	1.01	0.00	4.32	–
STD	0.00	0.00	0.01	0.00	0.01	0.06	0.00	0.17	–

[a] Share of oligomers for the hydrolysate components according to Equation (2.7); [b]
[b] About 20 % of the hydrolysate volume.

is 7.9 ± 0.1 % after analytical hydrolysis. Highly volatile components (mainly acetic acid and the formed furfural) are lost via the gas phase (Table 3).

Discussion. It remains unclear whether the glucose is released from fragments of cellulose, parts of hemicellulose or from other plant components or intermediates. Another hypothesis is that methylglucoronic acid, which is typically found in hemicellulose of herbaceous biomass, co-elutes with glucose and cannot be differentiated by analytical methods described in section 2.4.2 (Ebringerová 2005). The highest share of oligomers (Equation (2.7)) indicates a higher stability of the glycosidic bonds for the glucose subunits in oligomers. The arabinose to xylose ratio (Ara/Xyl in Table 3) confirms that the oligomers in the hydrolysate are mainly composed of xylose subunits, as the main part of the arabinose is already present as monomers after steam treatment. This can be explained by the fact that arabinose mainly occurs in the side chains of the arabinoxylan and the α-3, 1- or α-2, 1-glycosidic bonds are less stable than the ß-1, 4-bonds between the xylose subunits of the xylan backbone (Ebringerová 2005; Ibbett et al., 2011). Parts of the hydrolysate components are degraded during primary hydrolysis and are lost via the gas phase, which is evident from the high concentration of furfural in the condensate (Table 3). It is important to emphasize that intermediate goals were achieved with the described approach (2.2.1). The setup enables an effective hydrolysis of the hemicellulose (about 63 %) without intensive degradation reactions. As a result, the main part of the xylose (87 %) is recovered in the form of XOS/WSX and the majority of the cellulose and lignin fraction remains in the solid residue.

3.1.3. Ultrafiltration

Results. The aim of the ultrafiltration studies was to evaluate selected membranes for the separation of xylooligosaccharides (XOS) / water soluble xylans (WSX) based on characteristic values (Fig. 1) according to the methods described in section 2.3. In the following, the results regarding the characteristic values in section 2.3.2 are summarized in Fig. 4A to Fig. 4E and then discussed.

3.1.4. Permeability

Results. Fig. 4A shows the mean values of permeabilities for the filtration of deionized water compared to hydrolysate sample for the membranes studied, each from triplicate determination with standard deviations (STD). It is noticeable that the UH30 membrane made of hydrophilized Polyethersulfone has a much lower permeability for deionized water than membranes with smaller pore sizes (UP20, UP10 and UF10). The permeabilities for deionized water of most membranes range from 37 to 123 L/(m^2 h bar). The values for membranes UP5 and UH4 are remarkably low in comparison (11.9 and 8.7 L/(m^2 h bar)), while the values for membrane UH50 are noticeably high (1907 L/(m^2 h bar)). The two membranes made of polyethersulfone (PES5 and PES10) show similar behavior in the filtration of deionized water and the sample despite different MWCOs. For the filtration of the hydrolysate, the permeabilities of all membranes, except UH50, reduce significantly (resulting in permeabilities from 1.0 to 7.4 L/(m^2 h bar)). The result of membrane UH4 is remarkable. The permeability during filtration of the sample in comparison with UP5 and UF5 membranes is 27 % and 40 % higher, respectively. The permeability of the UH50 membrane for the hydrolysate sample is on average 15 times higher than that of the second highest (UH30).

Discussion. The results clearly show that the permeability of the membranes is not completely dependent on the respective pore size. The significantly lower permeability of the UH30 membrane compared with the UP20 and even the UP10 for deionized water cannot be explained by the MWCO alone. The considerable differences in permeability for deionized water between the UP5 and UF5 membranes cannot be attributed to the MWCO either. One possible explanation for the results is that in ultrafiltration, material properties such as surface charge (zeta potential) and hydrophobicity also play an important role (Mantel et al., 2018). The results show that there are interactions with the hydrolysate that strongly influence the decrease in permeability (especially with less hydrophilic materials) in some cases. Consequently, process effort and the success of ultrafiltration in downstreaming also depend to a considerable extent on the choice of a membrane (material) suitable for hemicellulose hydrolysates from wheat straw. In this case, the hydrophilized materials show the best results, due to the comparatively low relative loss of permeability during filtration of the sample.

3.1.5. Carbohydrates rejection

Results. The results summed up in Fig. 4B show that there is no enrichment of non-monomeric xylose (i.e., xylooligosaccharides (XOS) / water soluble xylans (WSX)) in the retentate of UH50. The content of non-monomeric xylose in both phases is scarcely different from that in the feed, which means that this fraction can permeate freely through the membrane. The results of all other membranes in Fig. 4B show that the target fraction can be enriched in the retentate. As expected, the rejection (retention of the components according to Equation (2.12)) proceeds antiproportionally to the MWCO of the respective membrane and is maximum for UP5 and UF5 at about 81 %. However, the highest relative mean content of XOS/WSX was measured in the retentates of UH4, although the rejection is lower (73 %).

Discussion. The high permeability of UH50 for the hydrolysate can be explained by the fact that the target fraction (non-monomeric xylose) is obviously not retained. Thus, it can be stated that the (reversible) loss of permeability (Fig. 4A) is due to impurities larger than 50 kDa but not belonging to the target fraction that makes up the major part of the dry mass in the hydrolysate (Table 2). The measured differences to the relative 100 % non-monomeric xylose content expected (in the retentate

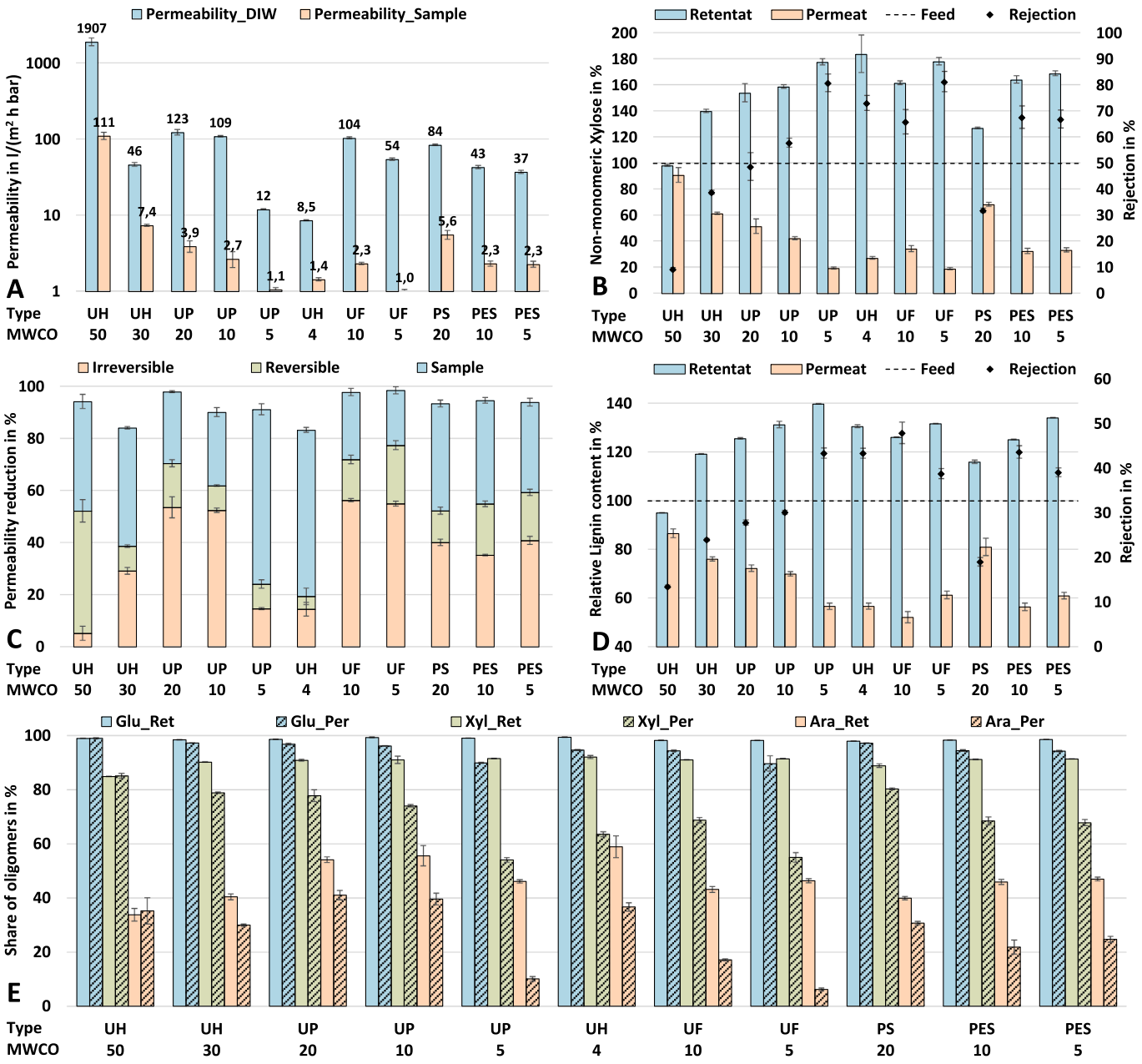

Fig. 4. Mean values from triplicates with standard deviations as error bars for: **A**: Permeability during filtration of deionized water (DIW) with virgin membranes and average permeability during filtration of the samples (hydrolysate). **B**: The relative content of non-monomeric xylose in permeates and retentates (left) and the corresponding rejection (right). **C**: Reversible, irreversible and sample caused reduction of the permeability (fouling). **D**: The relative lignin content in permeates and retentates (left) and the corresponding rejection (right). **E**: The share of oligomers of glucose (Glu), xylose (Xyl) and arabinose (Ara) in retentate (Ret) and permeate (Per) (hatched).

and especially in the permeate) are likely due to losses at the membrane and in the dead volume (tubes, spacers, etc.). Under these conditions, a rejection of 0 % is expected for non-monomeric xylose. However, the rejection is slightly increased by the losses and is about 9 %. The lower rejection of UH4 is due to the higher concentration of non-monomeric xylose in the permeate compared to UP5 and UF5, as less material is probably adsorbed on the hydrophilized surface of UH4 (Equation (2.12)). The distribution of the membrane rejection values over membranes also provides information about the approximate XOS/WSX molecule weight. In this context the rejection of 73 % for the UH4 means that under the set conditions about 27 % of the XOS/WSX in the hydrolysate are smaller than 4 kDa. The results indicate that some of the xylose-based biopolymers have a molar mass greater than 30 kDa, but the molar mass always appears to be less than 50 kDa.

3.1.6. *Fouling*

Results. Fig. 4C shows the results with respect to the fouling behavior of the investigated membranes. Here the losses of permeability are shown in relation to the initial deionized water permeability of the fresh membranes. For the reduction, three different types are differentiated. The results show that the membranes with hydrophilized active layer (UH) have by far the lowest potential for irreversible fouling. Moreover, the overall reduction of permeability during filtration of the sample is also low for the most hydrophilic membranes (UH30 & UH4). The percentages for mechanically irreversible fouling vary between 5 and 56 %. The UH50 with 5 % and the UP5 and UH4 with 14 % each show the lowest potential for irreversible fouling. The performance of UP5 shows similar behavior to the hydrophilized membranes with respect to all parameters studied. Beside this, the UP and UF membranes

are very susceptible to irreversible fouling, losing between 90 and 99 % of their initial permeability upon filtration of the hydrolysate. The overall reduction of permeability for UF10 and UF5 is 98 % and 99 %, respectively, of which 56 % and 55 % are irreversible.

Discussion. From the point of view of process technology, the lowest possible fouling is the goal. In particular, irreversible fouling (via backwashing) should be as small as possible, since it increases the operating pressure and / or membrane areas and shortens the service life of the membrane modules. The UF membrane type material is apparently particularly susceptible to fouling, which also accounts for the 50-fold reduction in permeability (Fig. 4A). This is probably due to the rather hydrophobic surface of the active layer of PS/PES. Nonpolar foulants such as lignin compounds (especially unsaturated carbon) can adsorb more effectively on hydrophobic surfaces (Nitzsche et al., 2022). In general, the reduction of the flow rates during filtration mainly results from concentration polarization, the formation of a secondary membrane / gel layer and the adsorption (of the more hydrophilic xylans as well) (Valério et al., 2021). A high percentage of irreversible fouling tends to indicate greater adsorption of foulants that cannot be removed mechanically (by backwashing). This can be seen, for example, for the UP and UF type membranes. A high percentage of reversible fouling points more to the formation of a secondary membrane or gel layer and blocking of the pores, which can be observed for membranes UH50, UP5 and UH4 (Fig. 4C). The sum of the effects is responsible for the decrease in permeability during filtration of the sample (Fig. 4A). In addition, increasing concentration polarization and viscosity (i.e., enrichment of biopolymers) contribute to the decline here. The considerable differences in fouling behavior may also be explained by interactions between the charges of the components in the hydrolysate and the membrane. In this case, the zeta potential of the components is typically investigated, which is of great importance for the membrane performance (Mantel et al., 2018). In this work, however, the zeta potential was not investigated.

3.1.7. Lignin rejection

Results. The results of lignin rejection are shown in Fig. 4D. The distribution of lignin contents shows that soluble lignin (i.e., phenolic compounds) is not completely free to permeate. All membranes with a MWCO below 50 kDa retain parts of the lignin, as phenolic compounds accumulate in the retentate. Qualitatively, the pattern follows the distribution of non-monomeric xylose (Fig. 4B), but quantitatively, significant differences are evident. Rejection for soluble lignin is much lower compared to xylooligosaccharides (XOS) / water soluble xylans (WSX), ranging from 13 % (UH50) to 48 % (UF10). The losses of water-soluble lignin (i.e., difference of detected lignin in feed and permeate + retentate), which cannot be recovered analytically, are between 0 % (UP10) and 11 % of the total measurable lignin content in the hydrolysate. For the membranes UH50 and PES10, the losses are 9 % each and maximum for the UF10 with 11 %. For membranes UH4 and UP5, the analytical losses are small and the analytical recoveries are 94 % and 98 %, respectively. The rejections for lignin range from 13 (UH50) to 48 % (UF10). The rejections correlate with the MWCO of the membranes.

Discussion. Lignin and its components are significant foulants and impurities in lignocellulose hydrolysates. Thus, one goal of the ultrafiltration is to separate impurities such as soluble lignin dissolved during primary hydrolysis from the target fraction. Since XOS/WSX are to be enriched in retentate (e.g., for subsequent separation via crystallization), low-molecular impurities such as soluble lignin are to remain in the permeate as far as possible. The results show that part of the lignin can be successfully separated, but the rejection values are biased upward by losses. For example, the expected value for UH50 is 0 % rejection, but the fouling losses cause a difference to the lignin content in the feed resulting in a falsified rejection according to Equation (2.12). Theoretically, at 0 % rejection, 100 % of the relative lignin content from the feed should be detected in the retentate and in the permeate. However, the sum of 200 % relative lignin content can only be stated for the UP10 membrane among the membranes examined. With all other membranes, the lignin from the feed cannot be completely recovered analytically, which is probably due to fouling and losses.

The results indicate a broad distribution of molar mass for a part of the dissolved phenolic components. The membranes UH4 and UP5 show that under the selected conditions about 56 % of the dissolved lignin in the hydrolysate suggest a molecular weight below 4 kDa and thus can permeate freely. The other part of the lignin is retained depending on the MWCO of the respective membrane. The results suggest two possible explanations. Either the remaining up to 44 % lignin actually has a higher molecular weight (between 4 kDa and 50 kDa) or it is bound to the oligomeric carbohydrates and is enriched in the retentate coupled to them.

3.1.8. Share of oligomers

Results. Fig. 4E shows the respective share of oligomers (S^{ol}) for the three main sugars glucose, xylose and arabinose according to Equation (2.7). For the UH50, no differences are seen between the two phases for all three sugars, since there is no effective separation. Thus, the distribution corresponds to the feed (Table 3). The results of the UP5 membrane are remarkable. Here (together with UF5), the largest differences between the two phases (permeate and retentate) are present. The share of oligomers for the glucose is consistently high at 90 % upward in all samples measured. Glucose is thus almost completely non-monomeric (with *DP* 2 up). However, the absolute amounts of non-monomeric glucose in the two phases (permeates and retentate) differ greatly after filtration. The ratios of measured glucose concentrations in permeate to retentate (c^{Per} / c^{Ret}) vary from 0.07 (for UP5 and UF5) to 0.90 (for UH50) due to the specific rejection (Equation (2.12)). The share of oligomeric arabinose is comparatively low (as already in the feed; Table 3) and ranges from 6 to 41 % in permeates and 34 to 59 % in retentates. The values for xylose (the main component of the target fraction) ranged from 54 to 85 % in the permeates and from 85 to 92 % in the retentates.

Discussion. The results show that the target fraction can be enriched and qualitatively be influenced by the choice of a suitable membrane. The oligomers in the permeate tend to be composed of low molecular weight carbohydrates (*DP* of 2 and above), while the high molecular weight carbohydrates tend to accumulate in the retentate. The low shares of oligomers in the permeates of membranes UP5 and UF5 (and thus the high differences) can possibly be attributed to different fouling mechanisms. In contrast to membrane UP5, the UF5 loses its permeability mainly due to adsorption of the nonpolar lignin components by irreversible fouling (Fig. 4C), thus its effective pore size is presumably smaller. The membrane UP5 behaves in the tests like a strongly hydrophilic membrane (i.e., low irreversible fouling). The share of oligomers indicates here a possible reason for the strong decrease in permeability of UP5 during filtration of the sample (Fig. 4A). Presumably, the retained oligomers accumulate on the surface of the membrane and thus form an additional resistance for the target fraction, whereby the effective pore size also appears to be smaller. According to the results, a broad molecular mass distribution between 342 Da to over 50 kDa is suggested for the glucose based oligosaccharides. Another hypothesis is that they are bound to xylan in side chains (e.g., as methylglucoronic acid that co-elutes with glucose), since the ratios (c^{Per} / c^{Ret}) of the measured xylan concentrations in the respective fraction are similar (Fig. 4B) (Ebringerová 2005).

3.2. Overall discussion

In the following, the results are discussed in the context of process development for the valorization of lignocellulose. In summary, the studies of primary hydrolysis with saturated steam show that the hemicellulose fraction of wheat straw can be selectively liquefied and separated from the solid phase (i.e., mainly cellulose and lignin) (Table 2). Based on the respective conditions, an almost particle-free

hydrolysate with comparatively few dissolved impurities is obtained (Table 2). Turbidity is an important indicator of the particle load in the samples (i.e., lignin, cellulose, cell debris, etc.) and thus of the effort required for downstreaming (especially by ultrafiltration). The turbidity of the hydrolysates directly after primary hydrolysis is in the range of 50 to 100 NTU. This indicates a comparatively low particle loading. After vacuum filtration (prefiltration with 5 μm; Fig. 1), turbidity typically drops to 1 to 5 NTU. This hydrolysate is well suited for a subsequent ultrafiltration since the hydrolysate contains mainly oligomeric hemicellulose in the dry mass and the impurities are of low molecular weight (Table 3). By means of ultrafiltration, several advantages can be realized at the same time - separation of the soluble low molecular impurities, enrichment of the oligomeric target fraction and a significant saving of (thermal) energy compared to thermal processes such as (vacuum) distillation.

The xylooligosaccharides (XOS) / water soluble xylans (WSX) contained in the hydrolysate can be effectively enriched and isolated from low molecular weight impurities even at moderate process conditions (20 °C and 1 to 4 bar transmembrane pressure). The low turbidity and the relatively high permeabilities (Fig. 4A) indicate a low fouling potential for the hydrolysate produced by the described pretreatment (section 2.2.1) compared to similar processes in the literature. Valerio et al. studied similar membranes for the ultrafiltration of arabinoxylans after alkaline extraction and observed permeabilities for the membrane UH50 that were about 40-fold lower despite higher ultrafiltration temperatures (Valério et al., 2021). Nitzsche et al. have found comparable flux rates for an ultrafiltration membrane with 1,000 – 3,500 Da MWCO; however, they used higher pressures and significantly higher temperatures. Furthermore, the concentrations of oligomers in the feed were lower compared to the feed used in this study. The hydrolysate was prepared hydrothermally using organic solvents and H_2SO_4 (i.e., more complex and expensive). In addition, considerable fouling effects continue to occur and the permeability decreases sharply, which is typical for hydrothermally treated hydrolysates (Nitzsche et al., 2022). However, the comparability is limited due to different test conditions. Nevertheless, the relatively high permeabilities at moderate experimental conditions shown indicate a potential for energy-efficient realization even on a larger scale. Higher temperatures or a higher pH value can further increase the permeability significantly, since the relationship is proportional.

The overarching motivation is to enable XOS/WSX production from hemicellulose as a byproduct of a continuous biorefinery (Scapini et al., 2021). All steps are designed for scalable and energy-efficient operation with as few auxiliary materials as possible. In the approach presented, only wastewater with components from the biomass is produced, parts of which can be recycled. There is no extensive preparation of the biomass before primary hydrolysis (supplementary data). The primary hydrolysis of the wet biomass takes place at moderate conditions (for thermal processes) and still leads to an effective solubilization of the hemicellulose (similar to liquid hot water) including the advantages of steam processes (Ruiz et al., 2020). Hemicellulose solubilization of 63.1 ± 3.1 % is higher than, for example, achieved with enzymatic hydrolysis after alkaline pretreatment of wheat straw (Rodríguez-Sanz et al., 2022). The recovery of XOS/WSX in the hydrolysate and wash effluent is respectively higher than achieved with a combination of hydrothermal pretreatment and alkaline ethanol extraction (Chen et al., 2018). A high biodegradability of the cellulose (i.e., biogas potential) is achieved (supplementary data), which has to be considered in a holistic evaluation. Considering the solubilization of cellulose and lignin and their possible losses in the wash effluent, the recovery in the solid residue is relatively high at over 90 % for cellulose and (due to particle losses) at over 70 % for lignin.

4. Conclusion

Saturated steam at 180 °C without subsequent explosion was successfully used to hydrolyze a major part of the hemicellulose in wheat straw. The following ultrafiltration led to the effective enrichment of the xylooligosaccharides and water-soluble xylans. Hydrolysis with saturated steam allows direct production of biopolymers and recovery of excess steam. Ultrafiltration enables purification and separation of the target fraction. The combination of steaming and ultrafiltration is a comparatively simple approach for a continuous process and enables potential energy savings and economic benefits. The approach is strongly dependent on a suitable hydrophilic membrane (4 kDa MWCO or lower for high recoveries).

CRediT authorship contribution statement

Stanislav Parsin: Conceptualization, Methodology, Investigation, Data curation, Writing – original draft, Writing – review & editing, Visualization, Project administration. **Martin Kaltschmitt:** Supervision, Project administration, Funding acquisition.

Declaration of Competing Interest

The authors declare that they have no known competing financial interests or personal relationships that could have appeared to influence the work reported in this paper.

Data availability

Data will be made available on request.

Acknowledgement

We would like to thank the editorial board and the anonymous reviewers for their valuable assistance. Furthermore, we thank Marc Conrad, Marvin Scherzinger, Timo Steinbrecher and Andreas Zimmermann for their support and scientific collaboration. Funding: This work was supported by the German Federal Ministry of Education and Research (grant number: 031B0660F).

Appendix A. Supplementary data

Supplementary data to this article can be found online at https://doi.org/10.1016/j.biortech.2023.130071.

References

Aachary, A., 2011. Xylooligosaccharides (XOS) as an emerging prebiotic: microbial synthesis, utilization, structural characterization, bioactive properties, and applications. Comprehensive Rev. Food Sci. Food Safety 10 (1), 2–16. https://doi.org/10.1111/j.1541-4337.2010.00135.x.

Agbor, G., Vinson, J.A., Donnelly, P.E. (2014): Folin-Ciocalteau Reagent for Polyphenolic Assay. In IJFS, pp. 147–156. DOI: 10.19070/2326-3350-1400028.

Amorim, C., Silvério, S.C., Prather, K.L.J., Rodrigues, L.R., 2019. From lignocellulosic residues to market: production and commercial potential of xylooligosaccharides. Biotech. Adv. 37 (7), 107397 https://doi.org/10.1016/j.biotechadv.2019.05.003.

Andersen, L., 2022. Biogas production from straw—the challenge feedstock pretreatment. Biomass Conv. Bioref. 12 (2), 379–402. https://doi.org/10.1007/s13399-020-00740-y.

Beckendorff, A., Lamp, A., Kaltschmitt, M., 2021. Optimization of hydrolysis conditions for xylans and straw hydrolysates by HPLC analysis. Biomass Conv. Bioref. 1–14. https://doi.org/10.1007/s13399-021-01429-6.

Bhutto, A., et al., 2017. Insight into progress in pre-treatment of lignocellulosic biomass. Energy 122, 724–745. https://doi.org/10.1016/j.energy.2017.01.005.

Biswas, A., 2011. Steam pretreatment of Salix to upgrade biomass fuel for wood pellet production. Fuel Processing Tech. 92 (9), 1711–1717. https://doi.org/10.1016/j.fuproc.2011.04.017.

Brownell, H.H., Saddler, J.N., 1987. Steam pretreatment of lignocellulosic material for enhanced enzymatic hydrolysis. Biotech. Bioeng. 29 (2), 228–235. https://doi.org/10.1002/bit.260290213.

Carvalheiro, F., Duarte, L.C., Gírio, F.M., 2008. Hemicellulose biorefineries: a review on biomass pretreatments. Available online at J. Sci. Ind. Res. 67, 849–864. http://nopr.niscpr.res.in/handle/123456789/2429.

Chen, X., Li, H., Sun, S., Cao, X., Sun, R., 2018. Co-production of oligosaccharides and fermentable sugar from wheat straw by hydrothermal pretreatment combined with

alkaline ethanol extraction. Industrial Crops and Products 111, 78–85. https://doi.org/10.1016/j.indcrop.2017.10.014.
Diedrich, H., 2019. NCHS-elementaranalyse. M02.001. With assistance of Heike Frerichs Alina Stahl. Technische Universität Hamburg, Zentrallabor Chemische Analytik. checked on 10/25/2022 Available Online at. https://www.tuhh.de/zentrallabor/methoden/ac-methoden/m02001.html,.
DIN EN ISO 18122:2016-03, Biogene Festbrennstoffe_- Bestimmung des Aschegehaltes (ISO_18122:2015); Deutsche Fassung EN_ISO_18122:2015.
Dogaris, I., Karapati, S., Mamma, D., Kalogeris, E., Kekos, D., 2009. Hydrothermal processing and enzymatic hydrolysis of sorghum bagasse for fermentable carbohydrates production. Bioresour. Tech. 100 (24), 6543–6549. https://doi.org/10.1016/j.biortech.2009.07.046.
Dotsenko, G., Meyer, A.S., Canibe, N., Thygesen, A., Nielsen, M., 2018. Enzymatic production of wheat and ryegrass derived xylooligosaccharides and evaluation of their in vitro effect on pig gut microbiota. Biomass Conv. Bioref. 8 (3), 497–507. https://doi.org/10.1007/s13399-017-0298-y.
Ebringerová, A., 2005. Structural diversity and application potential of hemicelluloses. Macromol. Symp. 232 (1), 1–12. https://doi.org/10.1002/masy.200551401.
François, I.E.J.A., Lescroart, O., Veraverbeke, W.S., Windey, K., Verbeke, K., Broekaert, W.F., 2014. Tolerance and the effect of high doses of wheat bran extract, containing arabinoxylan-oligosaccharides, and oligofructose on faecal output: a double-blind, randomised, placebo-controlled, cross-over trial. J. Nutri. Sci. 3, e49.
Gírio, F.M., Fonseca, C., Carvalheiro, F., Duarte, L.C., Marques, S., Bogel-Łukasik, R., 2010. Hemicelluloses for fuel ethanol: a review. Bioresour. Tech. 101 (13), 4775–4800. https://doi.org/10.1016/j.biortech.2010.01.088.
Gómez, B., Míguez, B., Veiga, A., Parajó, J., 2015. Production, purification, and in vitro evaluation of the prebiotic potential of arabinoxylooligosaccharides from brewer's spent grain. J. Agri. Food Chem. 63 (38), 8429–8438. https://doi.org/10.1021/acs.jafc.5b03132.
Hongzhang, C., Liying, L., 2007. Unpolluted fractionation of wheat straw by steam explosion and ethanol extraction. Bioresour. Tech. 98 (3), 666–676. https://doi.org/10.1016/j.biortech.2006.02.029.
Ibbett, R., Gaddipati, S., Davies, S., Hill, S., Tucker, G., 2011. The mechanisms of hydrothermal deconstruction of lignocellulose: new insights from thermal-analytical and complementary studies. Bioresour. Techn. 102 (19), 9272–9278. https://doi.org/10.1016/j.biortech.2011.06.044.
Jacquemin, L., Zeitoun, R., Sablayrolles, C., Pontalier, P.-Y., Rigal, L., 2012. Evaluation of the technical and environmental performances of extraction and purification processes of arabinoxylans from wheat straw and bran. Process Biochem. 47 (3), 373–380. https://doi.org/10.1016/j.procbio.2011.10.025.
Kim, J., 2016. A review on alkaline pretreatment technology for bioconversion of lignocellulosic biomass. Bioresour. Tech. 199, 42–48. https://doi.org/10.1016/j.biortech.2015.08.085.
Klemm, M., Kröger, M., Görsch, K., Müller-Langer, F., Majer, S., 2020. Fuel-driven biorefineries using hydrothermal processes. Chemie Ingenieur Technik 92 (11), 1653–1664. https://doi.org/10.1002/cite.202000093.
Li, J., Henriksson, G., Gellerstedt, G., 2005. Carbohydrate reactions during high-temperature steam treatment of aspen wood. Appl. Biochem. Biotechnol. 125 (3), 175–188. https://doi.org/10.1385/ABAB:125:3:175.
Li, J., Henriksson, G., Gellerstedt, G., 2007. Lignin depolymerization/repolymerization and its critical role for delignification of aspen wood by steam explosion. Bioresour. Tech. 98 (16), 3061–3068. https://doi.org/10.1016/j.biortech.2006.10.018.
Luo, X., Ma, X., Hu, H., Li, C., Cao, S., Huang, L., 2013. Kinetic study of pentosan solubility during heating and reacting processes of steam treatment of green bamboo. Bioresour. Tech. 130, 769–776. https://doi.org/10.1016/j.biortech.2012.12.088.
Mantel, T., Benne, P., Parsin, S., Ernst, M., 2018. Electro-Conductive composite gold-polyethersulfone-ultrafiltration-membrane: characterization of membrane and natural organic matter (NOM) filtration performance at different in-situ applied surface potentials. Membranes 8 (3). https://doi.org/10.3390/membranes8030064.
Modenbach, A.A., Nokes, S.E., 2012. The use of high-solids loadings in biomass pretreatment–a review. Biotech. Bioeng. 109 (6), 1430–1442. https://doi.org/10.1002/bit.24464.
Montané, D., Nabarlatz, D., Martorell, A., Torné-Fernández, V., Fierro, V., 2006. Removal of lignin and associated impurities from Xylo-oligosaccharides by activated carbon adsorption. Ind. Eng. Chem. Res. 45 (7), 2294–2302. https://doi.org/10.1021/ie051051d.
Naidu, D., 2018. Bio-based products from xylan: a review. Carbohydrate Polymers 179, 28–41. https://doi.org/10.1016/j.carbpol.2017.09.064.
Nitzsche, Roy; Etzold, Hendrik; Verges, Marlen; Gröngröft, Arne; Kraume, Matthias (2022): Demonstration and Assessment of Purification Cascades for the Separation and Valorization of Hemicellulose from Organosolv Beechwood Hydrolyzates. In Membranes 12 (1). DOI: 10.3390/membranes12010082.
Qaseem, M., 2021. Cell wall hemicellulose for sustainable industrial utilization. Renew. Sustain. Energy Rev. 144, 110996 https://doi.org/10.1016/j.rser.2021.110996.
Rodríguez, F., Sanchez, A., Parra, C., 2017. Role of steam explosion on enzymatic digestibility, xylan extraction, and lignin release of lignocellulosic biomass. ACS Sustain. Chem. Eng. 5 (6), 5234–5240. https://doi.org/10.1021/acssuschemeng.7b00580.
Rodríguez-Sanz, Andrea; Fuciños, Clara; Torrado, Ana M.; Rúa, María L. (2022): Extraction of the wheat straw hemicellulose fraction assisted by commercial endo-xylanases. Role of the accessory enzyme activities. In Industrial Crops and Products 179, p. 114655. DOI: 10.1016/j.indcrop.2022.114655.
Ruiz, H.A., Conrad, M., Sun, S.-N., Sanchez, A., Rocha, G.J.M., Romaní, A., et al., 2020. Engineering aspects of hydrothermal pretreatment: from batch to continuous operation, scale-up and pilot reactor under biorefinery concept. Bioresour. Tech. 299, 122685 https://doi.org/10.1016/j.biortech.2019.122685.
Santibáñez, L., Henríquez, C., Corro-Tejeda, R., Bernal, S., Armijo, B., Salazar, O., 2021. Xylooligosaccharides from lignocellulosic biomass: a comprehensive review. Carbohydrate Polymers 251, 117118. https://doi.org/10.1016/j.carbpol.2020.117118.
Scapini, T., Santos, D., Maicon, S.N., Bonatto, C., Wancura, J.H.C., Mulinari, J., Camargo, A.F., et al., 2021. Hydrothermal pretreatment of lignocellulosic biomass for hemicellulose recovery. Bioresour. Tech. 342, 126033 https://doi.org/10.1016/j.biortech.2021.126033.
Scherzinger, M., Kaltschmitt, M., 2021. Thermal pre-treatment options to enhance anaerobic digestibility – a review. Renew. Sustain. Energy Rev. 137, 110627 https://doi.org/10.1016/j.rser.2020.110627.
Schütt, F., Westereng, B., Horn, S.J., Puls, J., Saake, B., 2012. Steam refining as an alternative to steam explosion. Bioresour. Tech. 111, 476–481. https://doi.org/10.1016/j.biortech.2012.02.011.
Sluiter, A., Hames, B., Ruiz, R., Scarlata, C., Sluiter, J., Templeton, D., Crocker, D., NREL: Determination of Structural Carbohydrates and Lignin in Biomass: Laboratory Analytical Procedure (LAP); Issue Date: April 2008; Revision Date: July 2011 (Version 07-08-2011).
Sluiter, A. (2008): Determination of Sugars, Byproducts, and Degradation Products in Liquid Fraction Process Samples: Laboratory Analytical Procedure (LAP); Issue Date: 12/08/2006. In Technical Report, p. 14.
So, D., Yao, C.u.K., Gill, P.A., Pillai, N., Gibson, P.R., Muir, J.G., 2021. Screening dietary fibres for fermentation characteristics and metabolic profiles using a rapid in vitro approach: implications for irritable bowel syndrome. British Journal of Nutrition 126 (2), 208–218. https://doi.org/10.1017/S0007114520003943.
Steinbrecher, T., Bonk, F., Scherzinger, M., Lüdtke, O., Kaltschmitt, M., 2022. Fractionation of lignocellulosic fibrous straw digestate by combined hydrothermal and enzymatic treatment. Energies 15 (17), 6111. https://doi.org/10.3390/en15176111.
Sun, X.F., Xu, F., Sun, R.C., Geng, Z.C., Fowler, P., Baird, M.S., 2005. Characteristics of degraded hemicellulosic polymers obtained from steam exploded wheat straw. Carbohydrate Polymers 60 (1), 15–26. https://doi.org/10.1016/j.carbpol.2004.11.012.
Valério, R., Crespo, J.G., Galinha, C.F., Brazinha, C., 2021. Effect of ultrafiltration operating conditions for separation of ferulic acid from arabinoxylans in corn fibre alkaline extract. Sustainability 13 (9), 4682. https://doi.org/10.3390/su13094682.
Wang, L., Littlewood, J., Murphy, R.J., 2013. Environmental sustainability of bioethanol production from wheat straw in the UK. Renew. Sustain. Energy Rev. 28, 715–725. https://doi.org/10.1016/j.rser.2013.08.031.
Zabed, H., Sahu, J.N., Boyce, A.N., Faruq, G., 2016. Fuel ethanol production from lignocellulosic biomass: an overview on feedstocks and technological approaches. Renew. Sustain. Energy Rev. 66, 751–774. https://doi.org/10.1016/j.rser.2016.08.038.